AIAA JOURNAL
Vol. 37, No. 4, April 1999

Coupled Thermoelasticity of Shells of Revolution: Effect of Normal Stress and Coupling

M. R. Eslami,* M. Shakeri,† A. R. Ohadi,‡ and B. Shiari‡
Amirkabir University of Technology, 15914 Tehran, Iran

The coupled thermoelasticity of shells of revolution, based on second-order shell theory, is considered, and the governing equations including normal stress and strain as well as the transverse shear and rotary inertia are considered. The coupled energy equation based on the assumption of Lord and Shulman (Lord, H. W., and Shulman, Y., "A Generalized Dynamical Theory of Thermoelasticity," *Journal of Mechanics and Physics of Solids*, Vol. 15, No. 5, 1967, pp. 299–309) is further considered, and the total system of equations is solved by means of Galerkin finite element method. It is concluded that the inclusion of normal stress in the coupled equation is significant and for thin shells can result in a noticeable difference in shell response compared to unassumed conditions.

Nomenclature

A_1, A_2	= first and second principal values
c_v	= specific heat at constant volume
E	= Young's modulus
G	= shear modulus
g_{ij}	= the components of metric tensor
h	= shell thickness
h_i, h_o	= convective coefficients
k	= conduction coefficient
L	= shell length
Q	= heat generation per unit mass
R_1, R_2	= principal radii of curvature
T_a	= reference temperature
u, v, w	= displacement components
α	= coefficient of thermal expansion
γ_{ij}	= shear strain tensor
ϵ_{ij}	= strain tensor
λ, μ	= Lamé constants
ν	= Poisson's ratio
ρ	= mass density
σ_{ij}	= stress tensor
τ_0	= relaxation time

I. Introduction

COUPLED thermoelasticity of shells was studied by McQuillen and Brull[1] who applied the traditional Galerkin method to thin cylindrical shells to obtain the approximate solution. First-order shell theory was considered, based on Love's assumptions, and the normal stress, transverse shear stress, and rotary inertia were essentially ignored, but a nonlinear temperature distribution was assumed across the shell thickness. They concluded that the difference between the coupled and uncoupled solutions is about 1%. Later, in 1982, Ghosn and Sabbaghian[2] presented an analytical solution for coupled thermoelasticity of thick cylinders based on the Laplace transform method. Li et al.[3] and Eslami and Vahedi[4] used the Galerkin finite element method and applied it to the coupled thermoelasticity of thick cylinders and spheres. Thin cylindrical shell under thermal shock was studied by Takazono et al.,[5] where the uncoupled equations of shell are considered, and viscoplasticity of shell is discussed. Hata[6] considered a thick spherical shell under thermal shock, and using analytical methods obtained the uncoupled dynamic thermoelastic stress waves. The coupled thermoelasticity of thin cylindrical shells was analyzed in Ref. 7, where the first-order shell theory based on the Love assumption was used, and the proper Galerkin finite element formulation was presented. Because the analysis was performed for long thin cylindrical shells, the axial displacement was ignored, and only the lateral shell displacement was considered in the analysis.

Shells under shock and impulsive loads tend to be sensitive to the normal stress. The thin shells response to the applied impulsive loads may differ significantly when normal stress is considered. The effect is far more than the consideration of the transverse shear and rotary inertia, which are occasionally considered to improve the accuracy. It is shown that even second-order shell theory is sensitive to the inclusion of normal stress for such types of loading.[8,9]

In this paper, the full stress–strain relations of three-dimensional elasticity is considered, and the Flugge second-order shell theory, which is the most complete compared to the other classical second-order theories, is employed to formulate the coupled thermoelasticity of shells of revolution. The results are obtained using a formulation where the normal stress is not considered. For the typical shell geometry and material properties, about 5% difference in shell response is observed. Furthermore, the effect of the coupling term is studied, and the results are compared for coupled and uncoupled equations.

II. Derivations

The basic assumption to consider the normal stress and strain in the shell equations requires relating the displacement components along the principal orthogonal curvilinear coordinate of shell to the displacement components on the middle plane as given by the following relations:

$$\begin{aligned} U(\alpha_1, \alpha_2, z) &= u(\alpha_1, \alpha_2) + z\beta_1(\alpha_1, \alpha_2) \\ V(\alpha_1, \alpha_2, z) &= v(\alpha_1, \alpha_2) + z\beta_2(\alpha_1, \alpha_2) \\ W(\alpha_1, \alpha_2, z) &= w(\alpha_1, \alpha_2) + zw'(\alpha_1, \alpha_2) + (z^2/2)w''(\alpha_1, \alpha_2) \end{aligned} \tag{1}$$

where (α_1, α_2, z) are the principal orthogonal curvilinear coordinates of the shell (as shown in Fig. 1), u, v, and w are the middle plane displacements, β_1 and β_2 are rotations of the tangent line to the middle plane along the α_1 and α_2 axes, respectively, and w' and w'' are the nonzero transverse normal strain. Consideration of these two terms, w' and w'', violates Love's third assumption (which states $\gamma_n = 0$) and part of Love's forth assumption (which states $\epsilon_n = 0$). Furthermore, if the transverse shear strains γ_{1n} and γ_{2n} are not made zero, rotations β_1 and β_2 are no longer simply described in terms of the middle plane displacements, and the restrictions imposed by the other part of Love's forth assumption (which state $\gamma_{1n} = \gamma_{2n} = 0$) is removed. From the general strain-displacement relations in curvilinear coordinate in terms of the covarient derivative

Received Nov. 14, 1997; revision received June 29, 1998; accepted for publication Nov. 4, 1998.

*Professor, Mechanical Engineering Department, 424 Hafez Avenue. E-mail: eslami@cic.aku.ac.ir. Associate Fellow AIAA.

†Associate Professor, Mechanical Engineering Department, 424 Hafez Avenue.

‡Ph.D. Student, Mechanical Engineering Department, 424 Hafez Avenue.

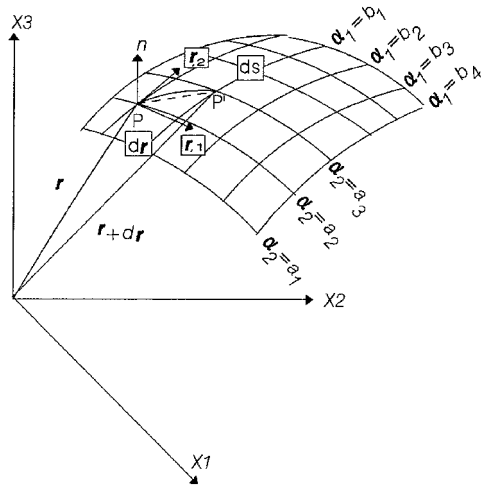

Fig. 1 Shell coordinate directions.

$$\epsilon_{ij} = \tfrac{1}{2}(U_i|_j + U_j|_i) \tag{2}$$

The strain-displacement relations for the second-order shell theory is as follows:

$$\epsilon_1 = \frac{1}{[1+(z/R_1)]}\left(\epsilon_1^0 + z\epsilon_1' + \frac{z^2}{2}\epsilon_1''\right)$$

$$\epsilon_2 = \frac{1}{[1+(z/R_2)]}\left(\epsilon_2^0 + z\epsilon_2' + \frac{z^2}{2}\epsilon_2''\right)$$

$$\epsilon_n = w' + zw''$$

$$\gamma_{1n} = \frac{1}{[1+(z/R_1)]}\left(\mu_1^0 + z\mu_1' + \frac{z^2}{2}\mu_1''\right) \tag{3}$$

$$\gamma_{2n} = \frac{1}{[1+(z/R_2)]}\left(\mu_2^0 + z\mu_2' + \frac{z^2}{2}\mu_2''\right)$$

$$\gamma_{12} = \frac{1}{[1+(z/R_1)]}\left(\beta_1^0 + z\beta_1'\right) + \frac{1}{[1+(z/R_2)]}\left(\beta_2^0 + z\beta_1'\right)$$

where the definition of the terms given in Eqs. (3) are

$$\epsilon_1^0 = \frac{1}{A_1}\frac{\partial u}{\partial \alpha_1} + \frac{v}{A_1A_2}\frac{\partial A_1}{\partial \alpha_2} + \frac{w}{R_1}$$

$$\epsilon_2^0 = \frac{1}{A_2}\frac{\partial v}{\partial \alpha_2} + \frac{u}{A_1A_2}\frac{\partial A_2}{\partial \alpha_1} + \frac{w}{R_2}$$

$$k_1 = \frac{1}{A_1}\frac{\partial \beta_1}{\partial \alpha_1} + \frac{\beta_2}{A_1A_2}\frac{\partial A_1}{\partial \alpha_2}, \qquad k_2 = \frac{1}{A_2}\frac{\partial \beta_2}{\partial \alpha_2} + \frac{\beta_1}{A_1A_2}\frac{\partial A_2}{\partial \alpha_1}$$

$$\beta_1^0 = \frac{1}{A_1}\frac{\partial v}{\partial \alpha_1} - \frac{u}{A_1A_2}\frac{\partial A_1}{\partial \alpha_2}, \qquad \beta_2^0 = \frac{1}{A_2}\frac{\partial u}{\partial \alpha_2} - \frac{v}{A_1A_2}\frac{\partial A_2}{\partial \alpha_1}$$

$$\beta_1' = \frac{1}{A_1}\frac{\partial \beta_2}{\partial \alpha_1} - \frac{\beta_1}{A_1A_2}\frac{\partial A_1}{\partial \alpha_2}, \qquad \beta_2' = \frac{1}{A_2}\frac{\partial \beta_1}{\partial \alpha_2} - \frac{\beta_2}{A_1A_2}\frac{\partial A_2}{\partial \alpha_1}$$

$$\mu_1^0 = \frac{1}{A_1}\frac{\partial w}{\partial \alpha_1} - \frac{u}{R_1} + \beta_1, \qquad \mu_1' = \frac{1}{A_1}\frac{\partial w'}{\partial \alpha_1} \tag{4}$$

$$\mu_1'' = \frac{1}{A_1}\frac{\partial w''}{\partial \alpha_1}, \qquad \mu_2^0 = \frac{1}{A_2}\frac{\partial w}{\partial \alpha_2} - \frac{v}{R_2} + \beta_2$$

$$\mu_2' = \frac{1}{A_2}\frac{\partial w'}{\partial \alpha_2}, \qquad \mu_1'' = \frac{1}{A_2}\frac{\partial w''}{\partial \alpha_2}$$

$$\epsilon_1' = k_1 + \frac{w'}{R_1}, \qquad \epsilon_2' = k_2 + \frac{w'}{R_2}$$

$$\epsilon_1'' = \frac{w''}{R_1}, \qquad \epsilon_2'' = \frac{w''}{R_2}$$

These relations are obtained based on Flugge's second-order shell theory, where the term z/R is retained in the equations compared to unity.

The forces and moments resultants based on second-order shell theory are defined as

$$\langle N_1, N_{12}, Q_1\rangle = \int_{-h}^{+h} (\sigma_1, \tau_{12}, \tau_{1n})\left(1+\frac{z}{R_2}\right)\mathrm{d}z$$

$$\langle N_2, N_{21}, Q_2\rangle = \int_{-h}^{+h} (\sigma_2, \tau_{12}, \tau_{2n})\left(1+\frac{z}{R_1}\right)\mathrm{d}z$$

$$\langle M_1, M_{12}\rangle = \int_{-h}^{+h} (\sigma_1, \tau_{12})\left(1+\frac{z}{R_2}\right)z\,\mathrm{d}z \tag{5}$$

$$\langle M_2, M_{21}\rangle = \int_{-h}^{+h} (\sigma_2, \tau_{21})\left(1+\frac{z}{R_1}\right)z\,\mathrm{d}z$$

$$\langle S_i, P_i, T_i\rangle = \frac{1}{2}\int_{-h}^{+h}\left(\tau_{in}, \frac{\sigma_n z^2}{2}, \frac{\tau_{in}z^2}{2}\right)\left(1+\frac{z}{R_1}\right)\mathrm{d}z$$

$$\langle A, B\rangle = \int_{-h}^{+h} (\sigma_n, \sigma_n z)\left(1+\frac{z}{R_1}\right)\left(1+\frac{z}{R_2}\right)\mathrm{d}z \qquad i, j = 1, 2$$

The temperature distribution across the shell thickness is assumed as

$$T(\alpha_1, \alpha_2, z, t) - T_a = T_0(\alpha_1, \alpha_2, t) + zT_1(\alpha_1, \alpha_2, t) \tag{6}$$

The equations of motion can be obtained using Hamilton's variational principal.[10]

For this general case, where the normal stress and strain are included in the governing equations, Hamilton's principal yields the following equations of motion:

$$\frac{\partial(A_2N_1)}{\partial\alpha_1} + \frac{\partial(A_1N_{21})}{\partial\alpha_2} + N_{12}\frac{\partial A_1}{\partial\alpha_2} - N_2\frac{\partial A_2}{\partial\alpha_1} + \frac{Q_1A_1A_2}{R_1}$$
$$+ A_1A_2\left\{q_1 - \rho h\left[\left(1+\frac{h^2}{12R_1R_2}\right)\ddot{u}\right.\right.$$
$$\left.\left. + \frac{h^2}{12}\left(\frac{1}{R_1}+\frac{1}{R_2}\right)\ddot{\beta}_1\right]\right\} = 0$$

$$\frac{\partial(A_1N_2)}{\partial\alpha_2} + \frac{\partial(A_2N_{12})}{\partial\alpha_1} + N_{21}\frac{\partial A_2}{\partial\alpha_1} - N_1\frac{\partial A_1}{\partial\alpha_2} + \frac{Q_2A_1A_2}{R_2}$$
$$+ A_1A_2\left\{q_2 - \rho h\left[\left(1+\frac{h^2}{12R_1R_2}\right)\ddot{v}\right.\right.$$
$$\left.\left. + \frac{h^2}{12}\left(\frac{1}{R_1}+\frac{1}{R_2}\right)\ddot{\beta}_2\right]\right\} = 0$$

$$\frac{\partial(A_2Q_1)}{\partial\alpha_1} + \frac{\partial(A_1Q_2)}{\partial\alpha_2} - A_1A_2\left(\frac{N_1}{R_1}+\frac{N_2}{R_2}\right)$$
$$+ A_1A_2\left\{-q_n - \rho h\left[\left(1+\frac{h^2}{12R_1R_2}\right)\ddot{w}\right.\right.$$
$$\left.\left. + \frac{h^2}{12}\left(\frac{1}{R_1}+\frac{1}{R_2}\right)\ddot{w}' + \frac{h^2}{24}\left(1+\frac{3h^2}{20R_1R_2}\ddot{w}''\right)\right]\right\} = 0$$

$$\frac{\partial(A_2M_1)}{\partial\alpha_1} + \frac{\partial(A_1M_{21})}{\partial\alpha_2} + M_{12}\frac{\partial A_1}{\partial\alpha_2} - M_2\frac{\partial A_2}{\partial\alpha_1}$$
$$- Q_1A_1A_2 + A_1A_2\left\{m_1 - \frac{\rho h^3}{12}\left[\left(\frac{1}{R_1}+\frac{1}{R_2}\right)\ddot{u}\right.\right.$$
$$\left.\left. + \left(1+\frac{3h^2}{20R_1R_2}\right)\ddot{\beta}_1\right]\right\} = 0$$

$$\frac{\partial(A_1M_2)}{\partial\alpha_2}+\frac{\partial(A_2M_{12})}{\partial\alpha_1}+M_{21}\frac{\partial A_2}{\partial\alpha_1}-M_1\frac{\partial A_1}{\partial\alpha_2}$$
$$-Q_2A_1A_2+A_1A_2\left\{m_2-\frac{\rho h^3}{12}\left[\left(\frac{1}{R_1}+\frac{1}{R_2}\right)\ddot{v}\right.\right.$$
$$\left.\left.+\left(1+\frac{3h^2}{20R_1R_2}\right)\ddot{\beta}_2\right]\right\}=0$$

$$\frac{\partial(A_2S_1)}{\partial\alpha_1}+\frac{\partial(A_1S_2)}{\partial\alpha_2}-A_1A_2\left(\frac{M_1}{R_1}+\frac{M_2}{R_2}\right)-AA_1A_2$$
$$+A_1A_2\left\{-m_n-\frac{\rho h^3}{12}\left[\left(\frac{1}{R_1}+\frac{1}{R_2}\right)\ddot{w}+\left(1+\frac{3h^2}{20R_1R_2}\right)\ddot{w}'\right.\right.$$
$$\left.\left.+\frac{3h^2}{40}\left(\frac{1}{R_1}+\frac{1}{R_2}\right)\ddot{w}''\right]\right\}=0$$

$$\frac{\partial(A_1T_2)}{\partial\alpha_2}+\frac{\partial(A_2T_1)}{\partial\alpha_1}-A_1A_2\left(\frac{P_1}{R_1}+\frac{P_2}{R_2}\right)-BA_1A_2$$
$$+A_1A_2\left\{-q_n\frac{h^2}{8}-\frac{\rho h^3}{24}\left[\left(1+\frac{3h^2}{20R_1R_2}\right)\ddot{w}\right.\right.$$
$$\left.\left.+\frac{3h^2}{20}\left(\frac{1}{R_1}+\frac{1}{R_2}\right)\ddot{w}'+\frac{3h^2}{40}\left(1+\frac{5h^2}{28R_1R_2}\right)\ddot{w}''\right]\right\}=0 \tag{7}$$

where (q_1, q_2, q_n) are the components of external force and (m_1, m_2, m_n) are the components of external moments acting on the middle plane of shell. These forces and moments are related to the external applied forces q_i^+ and q_i^- as

$$q_i=q_i^+[1+(z/R)]+q_i^-[1-(z/R)]$$
$$m_i=m_i^+[1+(z/R)]-m_i^-[1-(z/R)] \tag{8}$$

where q_i^+ acts on the outer surface and q_i^- acts on the inner surface of shell; q_n is selected positive in the opposite direction of normal to the middle plane. The sixth and seventh of Eqs. (7) are obtained due to the consideration of the normal stress and the introduction of parameters w' and w''.

There are seven independent natural boundary conditions that are to be used with the equations of motion and may be satisfied on the edge of shell. These conditions are as follows:

$$\begin{aligned}
&N_n=\bar{N}_n \quad \text{or} \quad u_n=\bar{u}_n\\
&N_{nt}=\bar{N}_{nt} \quad \text{or} \quad u_t=\bar{u}_t\\
&Q_n=\bar{Q}_n \quad \text{or} \quad w_n=\bar{w}_n\\
&M_n=\bar{M}_n \quad \text{or} \quad \beta_n=\bar{\beta}_n\\
&M_{nt}=\bar{M}_{nt} \quad \text{or} \quad \beta_t=\bar{\beta}_t\\
&S_n=\bar{S}_n \quad \text{or} \quad w_n'=\bar{w}_n'\\
&T_n=\bar{T}_n \quad \text{or} \quad w_n''=\bar{w}_n''
\end{aligned} \tag{9}$$

where the bar values are known and given on the boundary.

For the axisymmetric loading condition, the following simplifications are made:

$$v=\beta_2=\frac{\partial}{\partial\alpha_2}=\beta_1^0=\beta_2^0=\beta_1'=\beta_1''=\mu_2=\mu_2'=\mu_2''=0 \tag{10}$$

Substitution of these conditions into the strain displacement relations (3) and (4), with the help of Eqs. (5) and (6) and constitutive law, into the equation of motion (7) cause the second and fifth equations to be identically satisfied, and the equilibrium equations reduce to a set of five equations in terms of displacement components and rotations.

III. Energy Equation

When the time period of excitation or application of a thermal external agency t_T applied to a structure is comparable to the time period of structural disturbance t_s, thermal stress waves are produced, and the problem solution must be obtained through the coupled field. It is customary to introduce the strain tensor in the expression of entropy of continuum. This results in an expression for the conduction equation based on the first law of thermodynamics, which includes the first time rate of the strain tensor and temperature. We call the results the conventional coupled thermoelasticity theory. According to the conventional theory, the speed of propagation of thermal waves is infinity, which is physically not correct. Lord and Shulman[11] (L–S) and Green and Lindsay[12] resolved this discrepancy by suggesting the improved theory. The basis of the L–S theory is to substitute the Maxwell law for the classical Fourier law of conduction by introducing the relaxed time τ_0 in the constitutive law of heat conduction, and thus improve the energy equation by including the second rate of time of temperature and strain as follows:

$$K_{ij}T_{,ij}-\left(1+\tau_0\frac{\partial}{\partial t}\right)[c_v\rho\dot{T}+T_a\beta_{ij}\dot{\epsilon}_{ij}]=0 \tag{11}$$

In this paper we consider the L–S theory and adopt Eq. (11) for the energy equation. Considering a linear distribution of temperature across the shell thickness, as given by Eq. (6), two unknowns T_0 and T_1 appear in the energy equation. The following two integrals of the energy equation provides two independent energy equations for two independent functions T_0 and T_1 (Ref. 1):

$$\int_z(\text{residual})\times(1)\times dz=0 \tag{12}$$

$$\int_z(\text{residual})\times(z)\times dz=0 \tag{13}$$

The appendix gives the results of Eqs. (12) and (13) for spherical and cylindrical shells based on the shell theory derived in this paper.

IV. Galerkin Finite Element Formulation

The Galerkin finite element method is used to analyze the coupled thermoelastic shell equations. The nodal degrees of freedom for an axisymmetric coupled field are five shell variables u, w, ψ, w', and w'' and two temperature variables T_0 and T_1. It is verified that a linear test function for the shell variables provides a sufficiently accurate approximation compared to higher polynomials.[13] Considering identical shape functions for all seven degrees of freedom and applying the formal Galerkin method to the system of five shell equations and two energy equations (7), Eqs. (12) and (13) result in the following finite element equation:

$$[M]\{\ddot{d}\}+[C]\{\dot{d}\}+[K]\{d\}=\{F\} \tag{14}$$

where for the base element e

$$\langle d\rangle^e=\langle u \quad w \quad \psi \quad w' \quad w'' \quad T_0 \quad T_1\rangle \tag{15}$$

The force matrix is divided into two terms: One term is composed of the terms obtained through the weak formulation of the governing equations and the resulting natural boundary conditions, and the second term includes the components of external applied forces and thermal shocks. The process of weak formulation and terms that are selected for weak formulation in the governing equations is very important in regard to the resulting natural boundary conditions. The natural boundary conditions, which are obtained as the result of weak formulation, should either have a kinematical meaning on the boundary or add up to make a traction boundary condition. Therefore, it is essential to set up a possible kinematic and forced shell boundary conditions in advance and to try to obtain them by weak formulation. The set of boundary conditions presented in Eqs. (9) are obtained on the basis of this assumption.

The finite element equation of motion (14) may be solved in the time domain by many techniques, such as the Newmark, Houbolt, Wilson–θ, and other methods. In this paper the α method is used.

According to this method, the equation of motion (14) in time domain is transformed to the following form:

$$[M]\{a\}_{n+1} + (1+\alpha)[C]\{v\}_{n+1} - \alpha[C]\{v\}_n + (1+\alpha)[K]\{d\}_{n+1} - \alpha[K]\{d\}_n = \{F(t_{n+\alpha})\} \tag{16}$$

where $t_{n+\alpha} = (1+\alpha)t_{n+1} - \alpha t_n = t_{n+1} + \alpha\Delta t$. The α method becomes Newmark's method when $\alpha = 0$. The displacement and velocity matrices at time step $(n+1)$ is written in terms of their values at time step n as

$$\{d\}_{n+1} = \{d\}_n + \Delta t\{v\}_n + (\Delta t^2/2)[(1-2\beta)\{a\}_n + 2\beta\{a\}_{n+1}] \tag{17}$$

$$\{v\}_{n+1} = \{v\}_n + \Delta t[(1-\gamma)\{a\}_n + \gamma\{a\}_{n+1}] \tag{18}$$

where γ and β are the accuracy and stability parameters, respectively. Using Eqs. (17) and (18), we can obtain the unknown matrices $\{d\}_{n+1}$, $\{v\}_{n+1}$, and $\{a\}_{n+1}$ in terms of their values at t_n. Let us define the following matrices:

$$\{\bar{d}\}_{n+1} = \{d\}_n + \Delta t\{v\}_n + (\Delta t^2/2)(1-2\beta)\{a\}_n \tag{19}$$

$$\{\bar{v}\}_{n+1} = \{v\}_n + \Delta t(1-\gamma)\{a\}_n \tag{20}$$

From Eqs. (18) and (20)

$$\{a\}_{n+1} = \frac{1}{\beta(\Delta t)^2}[\{d\}_{n+1} - \{\bar{d}\}_{n+1}] \tag{21}$$

and from Eqs. (19) and (21)

$$\{v\}_{n+1} = \{\bar{v}\}_{n+1} + \frac{\gamma}{\beta(\Delta t)}[\{d\}_{n+1} - \{\bar{d}\}_{n+1}] \tag{22}$$

Substituting Eqs. (19–22) into Eq. (16), we obtain the main equation to solve for $\{d\}_{n+1}$:

$$\frac{1}{\beta(\Delta t)^2}[M] + (1+\alpha)\frac{\gamma}{\beta(\Delta t)}[C] + (1+\alpha)[K]\{d\}_{n+1} = \{F(t_{n+\alpha})\} - \left[\frac{1}{\beta(\Delta t)^2}[M] + (1+\alpha)\frac{\gamma}{\beta(\Delta t)}[C]\right]\{\bar{d}\}_{n+1} - (1+\alpha)[C]\{\bar{v}\}_{n+1} + \alpha[C]\{v\}_n + \alpha[K]\{d\}_n \tag{23}$$

The stable solution condition is not only based on the values of γ and β; it is also very sensitive to the choice of Δt. For the Newmark method, the values $2\beta > \gamma > \frac{1}{2}$ result in an unconditionally stable solution provided that the choice of Δt is correct. It is suggested that the following values are selected for the α method[14]:

$$\alpha \in \left[-\tfrac{1}{3}, 0\right], \qquad \gamma = (1-2\alpha)/2, \qquad \beta = [(1-2\alpha)/2]^2 \tag{24}$$

The numerical method will be unconditionally stable, will have second-order accuracy, and will self-initiate. Note that sometimes in the solution of Eq. (23) higher-frequency modes artificially appear, which do not belong to the equation. Therefore, it is required that these disturbing frequencies are deleted by increasing the artificial damping. This is possible using the α method because by decreasing the value of α the artificial numerical damping is increased without effecting the problem accuracy. The stability condition of the α method, similar to other methods, such as the Newmark, is based on the positive definite matrices. The application of the Galerkin method to this problem results in nonaxisymmetric stiffness and damping matrices, and therefore the resulting solution must be checked for its convergency. The selection of the time increment is important and has an absolute effect on solution convergency and accuracy.

V. Results

Consider a thin cylindrical shell of clamped edges with the geometrical and material properties given in Table 1.

The thermal conditions at the ends of the shell are assumed isolated, and the shell is considered to be exposed to the inside thermal shock given by the following equation:

$$T_i(t) = 2207(1 - e^{-13,100t}) + 293 \tag{25}$$

Table 1 Geometry and material properties of cylindrical shell

Parameter	Value
E	200 GN/m^2
k	50 W/m K
α	17.8×10^{-6} 1/K
L	0.40 m
R	0.1085 m
ν	0.3
ρ	7,904 kg/m^2
h	0.002 m
c_v	500 J/kg K
h_i	10,000 W/m^2 K
h_o	200 W/m^2 K
T_a	293 K

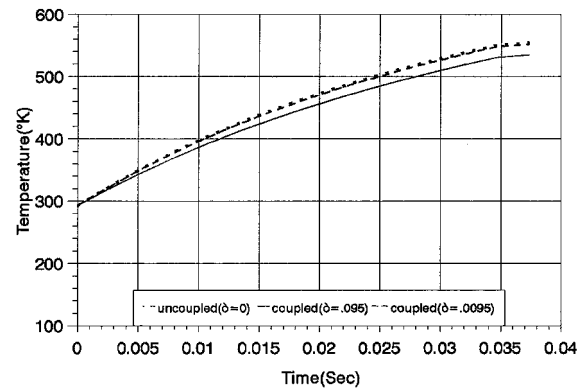

Fig. 2 Inside temperature vs time, example 1.

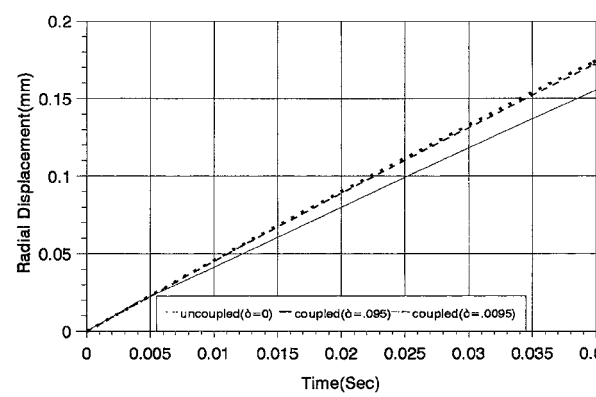

Fig. 3 Middle plane lateral deflection, example 1.

The temperature of the inside surface rises from 293 to 2500 K in 0.45 ms; the shell behavior is studied up to 0.04 s, which is about 90 times the time period required for the thermal shock to reach its steady-state condition. The shell is divided into 50 elements along its length, and the time increment is $1E-6$ s. In Fig. 2 the inside temperature vs time for the shell middle length is shown. The effect of mechanical coupling $\delta = [(1+\nu)\alpha^2 T_a E/(1-\nu)(1-2\nu)\rho c_v]$ is shown in Fig. 2. For $\delta = 0$, the mechanical coupling term from the energy is ignored, equation and the problem is decoupled. For the given shell $\delta = 0.0095$, it is noted that the effet of damping is negligible. For larger α or smaller c_v, the value of δ is larger. For $\delta = 0.095$, the mechanical coupling has a noticeable effect. In Fig. 3, this comparison is shown for the middle plane lateral deflection. It is noted that although at $t = 0.04$ s the thermal shock reached its steady-state condition, the lateral deflection and inside temperature are still increasing. The reason is that the characteristic time of heat transfer is much larger than the mechanical characteristic time for the stress wave. This behavior is different when the shell is under pressure shock.[9,15]

Now consider the same shell under low-rate thermal shock, as a second example. The equation of temperature shock applied to the cylindrical shell is

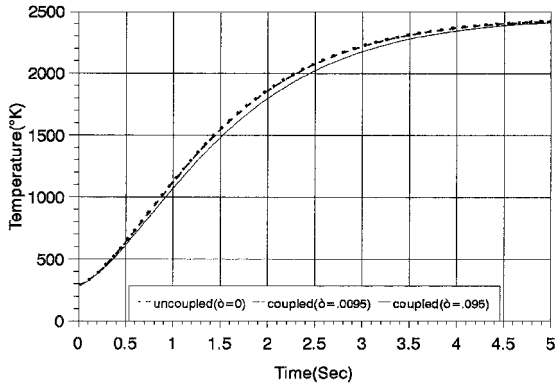

Fig. 4 Time history of inside surface temperature.

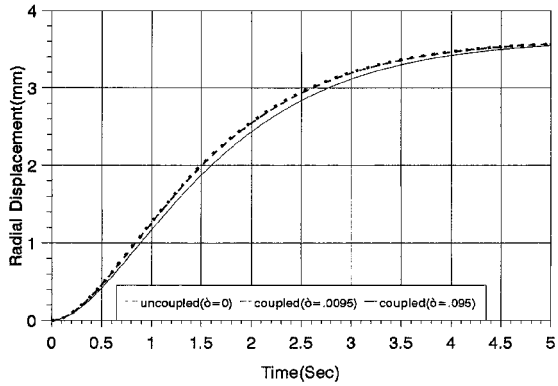

Fig. 5 Time history of radial displacement, example 2.

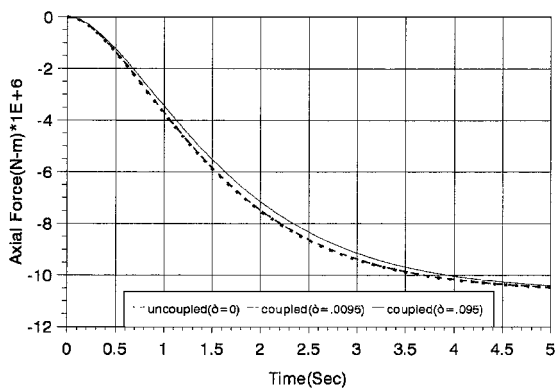

Fig. 6 Time history of axial force, example 2.

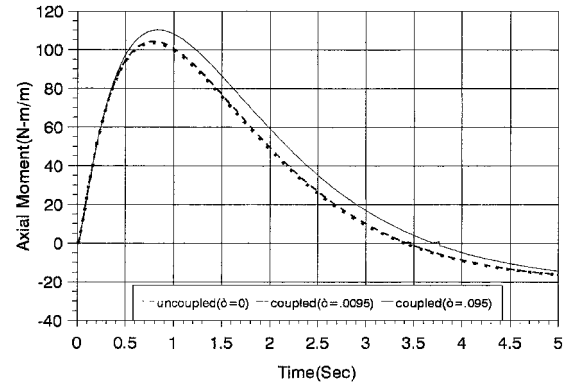

Fig. 7 Time history of axial moment, example 2.

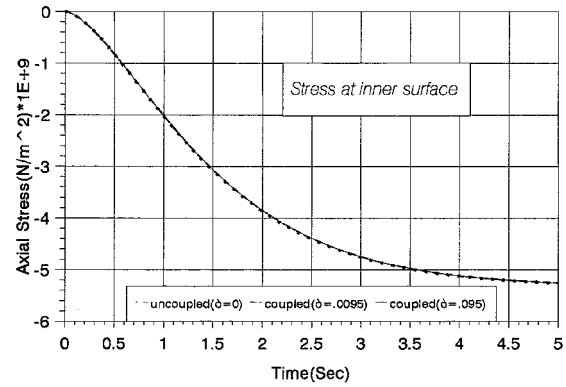

Fig. 8 Time history of axial stress at inner surface, example 2.

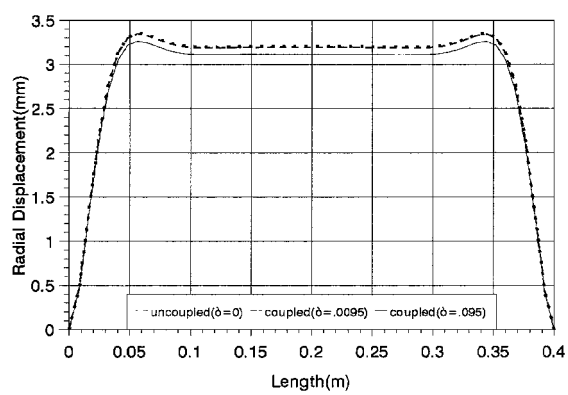

Fig. 9 Variation of radial displacement vs shell length, example 2.

$$T_i(t) = 2207(1 - e^{-1.3t}) + 293 \tag{26}$$

The rate of temperature (Kelvin) variation with respect to time is slower compared to Eq. (25). Temperature reaches to its maximum value within 3.5 s. The time increment is selected as $\Delta t = 0.01$ s, and the shell behavior is studied up to 5 s. It was observed that for $\Delta t = 0.005$, the results were negligibly different, and thus the selected value for Δt was justified. In Figs. 4 and 5, the time history of inside surface temperature and radial displacement of the shell middle length is shown. Similar to Figs. 2 and 3, the values of temperature and displacement for coupled condition ($\delta = 0.095$) are less than the values for semicoupled condition ($\delta = 0$). This means that the coupled effect acts like a damper, and thus it could be regarded as thermoelastic damping. At the beginning of the shock, due to lower values of strains, the difference between coupled ($\delta = 0.095$) and semicoupled ($\delta = 0$) is negligible, and as time increases this difference also increases. When temperature reaches its steady-state condition, the strains reach their maximum values while their time rate is decreased and the effect of mechanical coupling will also decrease. In Figs. 6–8 the time history of the axial force, axial moment, and axial stress at the inner surface are shown. Although both temperature and radial displacement are related to the axial force, because of their signs and coefficients, the effect of temperature is dominant, and the axial force is negative. Because the axial moment is small, the axial stress follows the pattern of the axial force. The variation of radial displacement, axial force, axial moment, and axial stress vs the shell length are shown in Figs. 9–12. In all of the figures describing the time history, the effect of mechanical coupling decreases as time increases, as expected.

The effect of normal stress is studied in the third example. A clamped edges cylindrical shell of $L = 1.0$ m, $R = 0.15$ m, $h = 0.005$ m, $E = 196$ GPa, $\rho = 8000$ kg/m^3, and $\nu = 0.3$ under inside uniform pressure shock of

$$P(t) = 8 \times 10^6(1 - e^{-13,100t}) \tag{27}$$

is considered. Pressure reaches its maximum value at 0.45 ms. Figure 13 shows the time history of the radial displacement of the middle length of the shell for two theories: when normal stress is considered (w is quadratic function of z) and when normal stress is not considered (w is constant across the thickness). Table 2 gives the radial displacement for the middle length at $t = 5E{-}4$ s. The

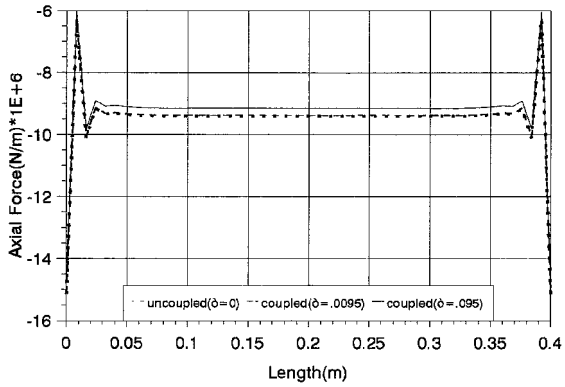

Fig. 10 Variation of axial force vs shell length, example 2.

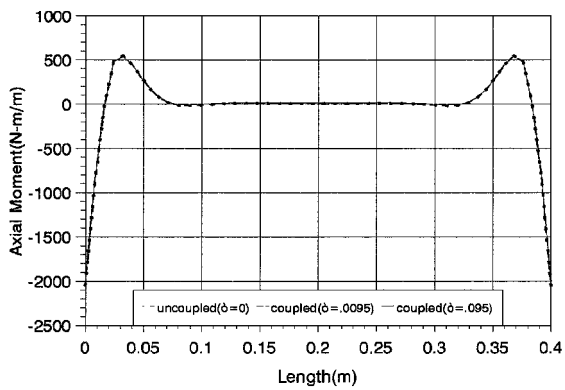

Fig. 11 Variation of axial moment vs shell length, example 2.

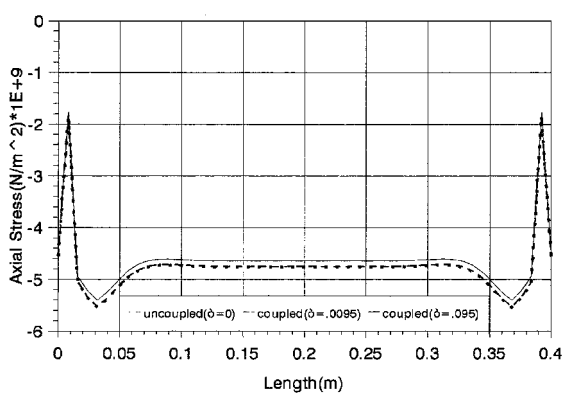

Fig. 12 Variation of axial stress vs shell length, example 2.

Table 2 Effect of normal stress (cylindrical shells)

Case	w, m $(R/h=30)$	w, m $(R/h=10)$
Theory including σ_n	$0.20976E-3$	$0.67291E-4$
Theory excluding σ_n	$0.20825E-3$	$0.65981E-4$
Percent of difference	0.7	2

difference between two cases is about 0.7% for $R/h = 30$ and 2% for $R/h = 10$.

In Fig. 14 the time history of the axial moment at the middle length of the shell for $R/h = 30$ is plotted. It is observed that the effect of normal stress causes a considerable increase of axial moment. Figure 15 shows the time history of normal stress for the middle length. At the inside surface, the normal stress is at equilibrium with the inside pressure, and at outside surface it is zero. Figures 16 and 17 show the time history of the axial force and moment at the middle length for $R/h = 10$. Figure 18 is a plot of the axial stress of the inside shell surface vs time at the same location for $R/h = 10$. The axial stress is the sum of $N_x/h + 12zM_x/h^3$. Because the axial force is dominant, the axial stress follows its pattern.

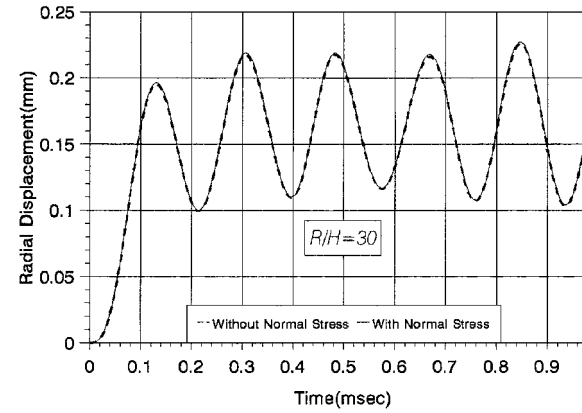

Fig. 13 Time history of radial displacement at middle length of shell for two theories, example 3.

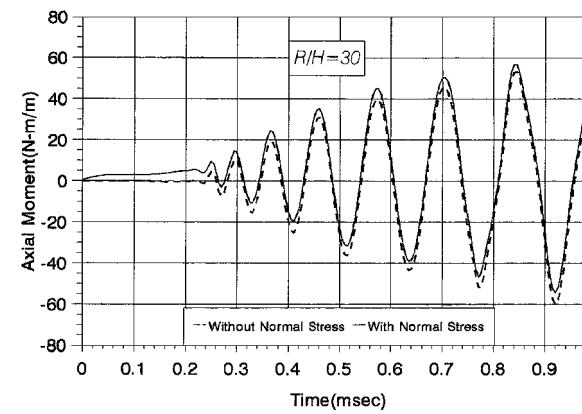

Fig. 14 Time history of axial moment at middle length of shell for $R/h = 30$, example 3.

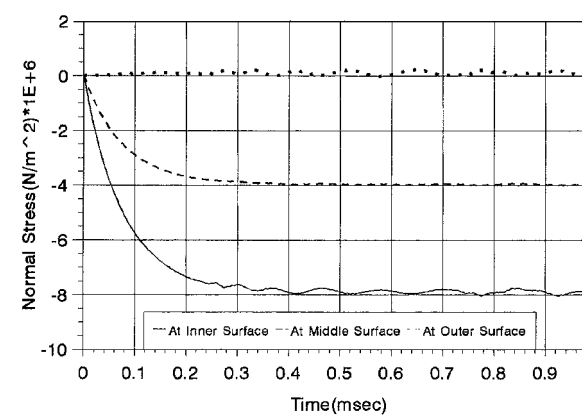

Fig. 15 Time history of normal stress for middle length, example 3.

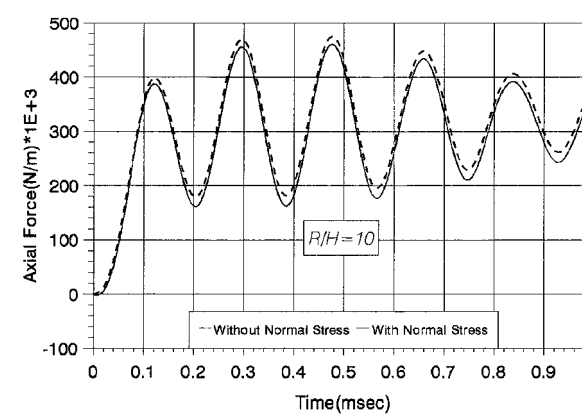

Fig. 16 Time history of axial force of inside shell surface at middle, example 3.

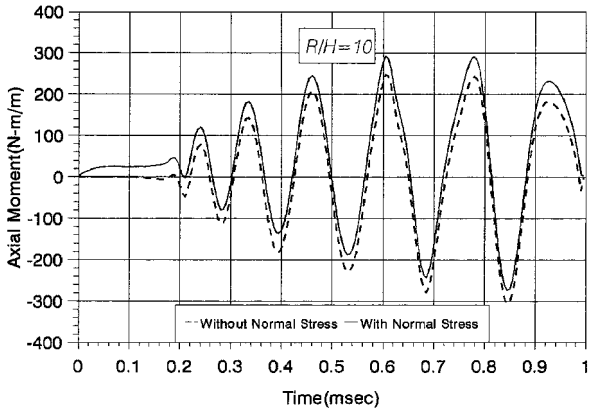

Fig. 17 Time history of axial moment of inside shell surface at middle length for $R/h = 10$, example 3.

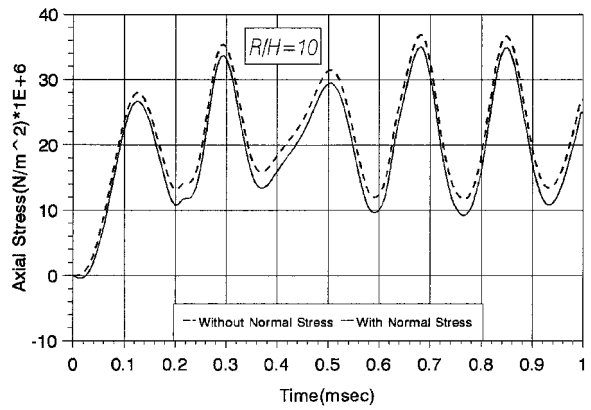

Fig. 18 Axial stress vs time at middle length for $R/h = 10$, example 3.

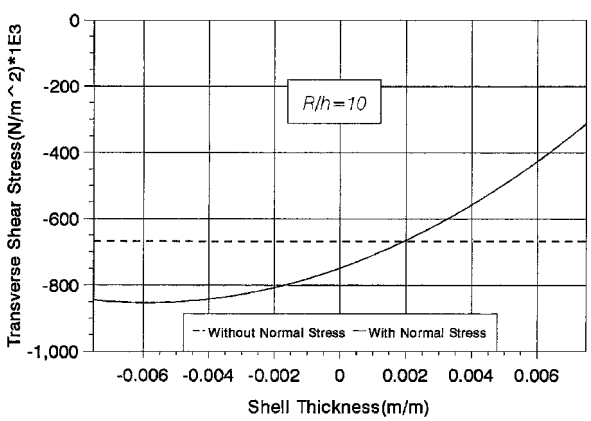

Fig. 19 Variation of shear stress vs shell thickness for $R/h = 10$, example 3.

The variation of transverse shear stress across the shell thickness is shown in Fig. 19. Figure 19 is for example 3 at $\frac{1}{8}L$ from the boundary and for $t = 0.8$ ms. The transverse shear at the shell middle length is negligible because the shell is relatively long. Note that when the normal stress is considered, the variation of shear stress across the thickness is nonlinear. However, it is expected that the shear stresses become zero on the inside and outside shell surfaces. This condition is in contradiction with the given nonzero shear stresses in Fig. 19. The reason for this error is that the boundary conditions of $\tau_{1n} = \tau_{2n} = 0$ at $z = \pm\frac{1}{2}$ h was not considered in the formulation. In Ref. 16, a method is suggested to resolve this problem, consideration of which results in a major change in the present formulation.

In Fig. 20, the variation of normal stress across the shell thickness is shown. Observe that the normal stress at the inside surface is $7.5E6$ Pa, smaller than the $8E6$ Pa of the inside pressure, and at outside surface it is roughly greater than zero, instead of being zero. The reason for this error is, again, not satisfying the exact boundary conditions of the normal stress on the inside and outside surfaces. The

Table 3 Effect of normal stress (spherical shells)

Case	w, m ($R/h = 30$)	w, m ($R/h = 10$)
Theory including σ_n	$1.731E-4$	$5.387E-5$
Theory excluding σ_n	$1.736E-4$	$5.634E-5$
Percent of difference	1.4	4.4

Table 4 Geometry and material properties of spherical shell

Parameter	Value
E	200 GN/m^2
R	0.15 m
h	0.015 m
h_o	200 W/m^2 K
k	50 W/mK
ν	0.3
c_v	500 J/kg K
G	76.9 GN/m^2
α_3	11.8×10^{-6} 1/K
ρ	7,904 kg/m^3
h_i	10,000 W/m^2 K
T_a	293 K

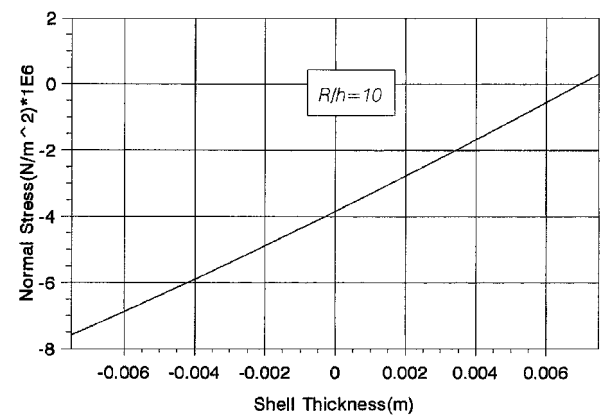

Fig. 20 Variation of normal stress vs shell thickness for $R/h = 10$, example 3.

method suggested in Ref. 16 can resolve this discrepancy without a major effect on the other results.

The fourth example is a spherical shell with the following data: $R = 0.3$ m, $h = 0.01$ m, $E = 200$ GPa, $\rho = 8000$ kg/m^3, and $\nu = 0.3$. The pressure pulse of Eq. (27) is applied, and the lateral deflection at the crown of the shell is given in Table 3 for $t = 0.6$ ms. Note that the consideration of normal stress improves the results up to 1.4% for $R/h = 30$, and 4.4% for $R/h = 10$.

The fifth example is a hemispherical shell with clamped edges under thermal shock given by Eq. (26) and the data given in Table 4.

In Figs. 21 and 22, the time history of the radial deflection and inside temperature at the crown of shell are given. It is noted that the mechanical coupling $\delta = 0.095$ has a considerable effect on shell response and causes the reduction of w and T. In Figs. 23–25 the time history of meridional force, moment, and stress of the same point is shown. Because the moment is dominant, the stress distribution follows its pattern. The positive moment of Fig. 24 causes compressive stress at the inside surface.

The final example is a cylindrical shell with clamped edges under thermal shock, given by Eq. 25 with the geometry and material properties given in Table 1. Figure 26 shows the difference between the values calculated under the two theories, the classical coupled theory ($\tau_0 = 0$) and L–S theory ($\tau_0 = 1.5 \times 10^{-6}$). The axial stress value for the L–S theory becomes smaller than for the classical theory. The maximum value of the difference is about 38%, which occurs at $t = 0.4 \times 10^{-3}$ s at the outer surface of the shell. Note that this difference between the two theories is due to the artificially increased value of τ_0, which for metallic material is about 1.6×10^{-12}.

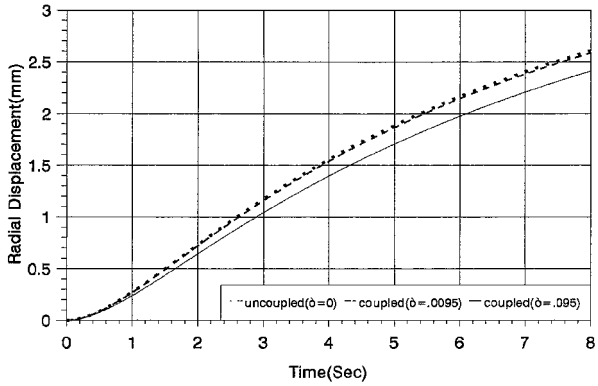

Fig. 21 The time history of radial deflection at the crown of shell, example 5.

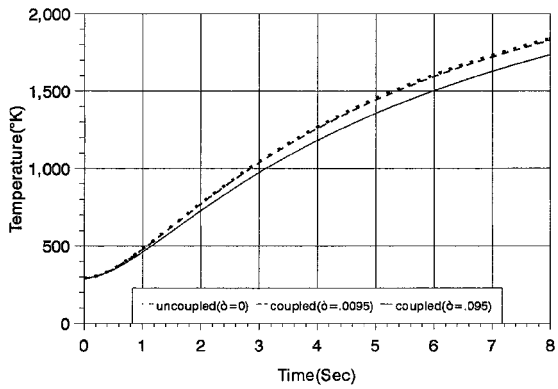

Fig. 22 Time history of inside temperature at the crown of shell, example 5.

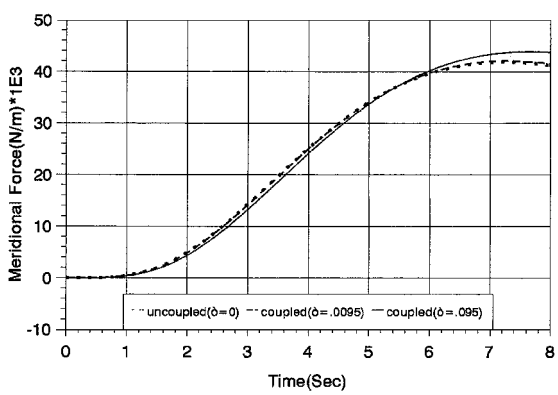

Fig. 23 Time history of meridional force at the crown of shell, example 5.

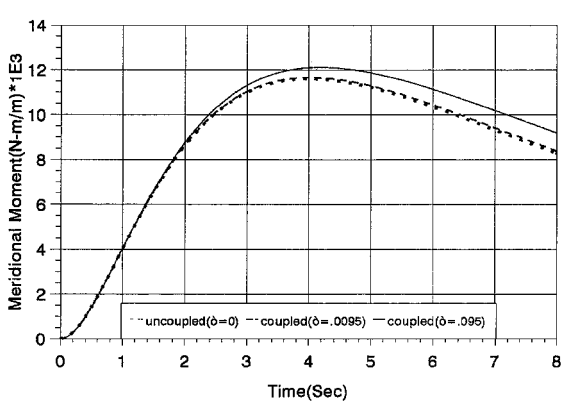

Fig. 24 Time history of meridional moment at the crown of shell, example 5.

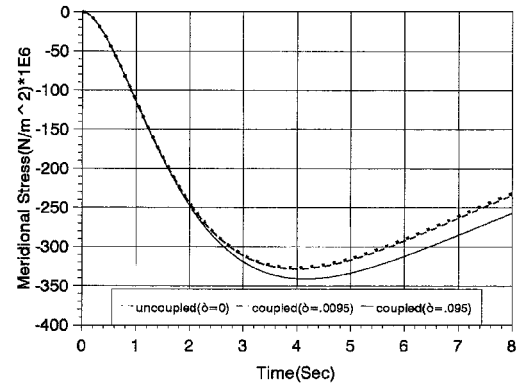

Fig. 25 Time history of meridional stress at the crown of shell, example 5.

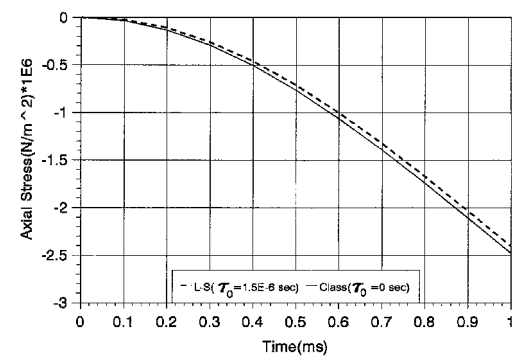

Fig. 26 Effect of τ_0 on axial stress derived under L–S theory in cylindrical shell, example 1.

VI. Conclusion

The shell response under thermal shock is defined through a set of thermoelastic equations coupled with the energy equation, provided that the thermal shock period is small enough compared to the time period characterizing the propagation of mechanical disturbances. The effect of the coupling is to predict smaller numerical values for temperature and displacement distribution along the shell, whereas the forces and moments are predicted to have higher values compared to the uncoupled formulations.

The effect of normal stress, when considered in the shell governing equations, is far more significant than the transverse shear stress, which is usually considered to impove the formulation's accuracy. The effect is magnified when the shell experiences high impulsive surface loads.

The second sound effect was checked for the shell response based on L–S theory. Consideration of the relaxation time results in prediction of higher values for axial stress distribution in the cylindrical shells.

Appendix: Results of Equations for Spherical and Cylindrical Shells

The energy equations for sphrical shells are

$$\frac{kh}{R^2}\frac{\partial^2 T_0}{\partial\phi^2}+\frac{kh}{R^2}\cot g\phi\frac{\partial T_0}{\partial\phi}-(h_i+h_o)T_0+\frac{h}{2}\left(h_i-h_0+\frac{4k}{R}\right)T_1$$

$$-(3\lambda+2\mu)\alpha T_a\left\{\left[\frac{h}{R}\cot g\phi\dot{u}+\frac{h}{R}\frac{\partial\dot{u}}{\partial\phi}+\frac{2h}{R}\dot{w}+h\dot{w}'\right.\right.$$

$$\left.+\frac{h^3}{12R}\dot{w}''\right]+\tau_0\left[\frac{h}{R}\cot g\phi\ddot{u}+\frac{h}{R}\frac{\partial\ddot{u}}{\partial\phi}+\frac{2h}{R}\ddot{w}+h\ddot{w}'\right.$$

$$\left.\left.+\frac{h^3}{12R}\ddot{w}''\right]\right\}-\rho c_v h(\dot{T}_0+\tau_0\ddot{T}_0)=-h_i[T_i(t)-T_a]$$

$$\frac{kh}{12R}\frac{\partial^2 T_1}{\partial\phi^2}+\frac{kh}{12R}\cot g\phi\frac{\partial T_1}{\partial\phi}-\frac{R}{2h}(h_i+h_o)T_0$$

$$-\left[\frac{R}{4}(h_i+h_o)+\frac{kR}{h}\right]T_1-(3\lambda+2\mu)\alpha T_a\left\{\left[\frac{h}{12}\cot g\phi\dot{\psi}\right.\right.$$

$$+\frac{h}{12}\frac{\partial\dot{\psi}}{\partial\phi}+\frac{2h}{R}\dot{w}+\frac{h}{6}\dot{w}'+\frac{Rh}{12}\ddot{w}''\Big]$$

$$\left.+\tau_0\left[\frac{h}{12}\cot g\phi\ddot{\psi}+\frac{h}{12}\frac{\partial\ddot{\Psi}}{\partial\phi}+\frac{h}{6}\ddot{w}'+\frac{Rh}{12}\ddot{w}''\right]\right\}$$

$$-\rho c_v\frac{Rh}{12}\dot{T}_1+\tau_0\ddot{T}_1=\frac{R}{2h}h_i[T_i(t)-T_a]$$

The energy equations for cylindrical shells are

$$kh\frac{\partial^2 T_0}{\partial x^2}-(h_i+h_o)T_0+\frac{h}{2}\left(h_i-h_0+\frac{2k}{R}\right)T_1$$

$$-(3\lambda+2\mu)\alpha T_a\left\{\left[h\frac{\partial\dot{u}}{\partial x}+\frac{h}{R}\dot{w}+h\dot{w}'+\frac{h^3}{24R}\ddot{w}''\right]\right.$$

$$\left.+\tau_0\left[h\frac{\partial\ddot{u}}{\partial x}+\frac{h}{R}\ddot{w}+h\ddot{w}'+\frac{h^3}{24R}\ddot{w}''\right]\right\}-\rho c_v h(\dot{T}_0+\tau_0\ddot{T}_0)$$

$$=-h_i[T_i(t)-T_a]$$

$$\frac{Rkh}{12}\frac{\partial^2 T_1}{\partial x^2}+-\frac{R}{2h}(h_i+h_o)T_0-\left[\frac{R}{4}(h_i-h_o)+\frac{kR}{h}\right]T_1$$

$$-(3\lambda+2\mu)\alpha T_a\left\{\left[\frac{Rh}{12}\frac{\partial\dot{\psi}}{\partial x}+\frac{h}{12}\dot{w}'+\frac{Rh}{12}\dot{w}''\right]+\tau_0\left[\frac{Rh}{12}\frac{\partial\ddot{\psi}}{\partial x}\right.\right.$$

$$\left.\left.+\frac{h}{12}\ddot{w}'+\frac{Rh}{12}\ddot{w}''\right]\right\}-\rho c_v\frac{Rh}{12}\dot{T}_1+\tau_0\ddot{T}_1=\frac{R}{2h}h_i[T_i(t)-T_a]$$

References

[1]McQuillen, E. J., and Brull, M. A., "Dynamic Thermoelastic Response of Cylindrical Shell," *Journal of Applied Mechanics*, Sept. 1970, pp. 661–670.

[2]Ghosn, A. H., and Sabbaghian, M., "Quasi-Static Coupled Problems of Thermoelasticity for Cylindrical Regions," *Journal of Thermal Stresses*, Vol. 5, 1982, pp. 253–280.

[3]Li, Y. Y., Ghoneim, H., and Chen, Y., "A Numerical Method in Solving a Coupled Thermoelasticity Equations and Some Results," *Journal of Thermal Stresses*, Vol. 6, 1983, pp. 253–280.

[4]Eslami, M. R., and Vahedi, H., "A Galerkin Finite Element Displacement Formulation of Coupled Thermoelasticity Spherical Problems," *Journal of Pressure Vessel Technology*, Vol. 114, No. 3, 1992, pp. 380–384.

[5]Takazono, S., Tao, K., and Taguchi, T., "Elasto/Viscoplastic Dynamic Response of Axisymmetric Shells Under Mechanical and/or Thermal Loading," *Proceedings of the ASME Pressure Vessel and Piping Conference* (Honolulu, HI), American Society of Mechanical Engineers, New York, 1989.

[6]Hata, T., "Thermal Shock in a Hollow Sphere Caused by Rapid Uniform Heating," *Journal of Applied Mechanics*, Vol. 58, No. 1, 1992, pp. 64–69.

[7]Eslami, M. R., Shakeri, M., and Sedaghati, R., "Coupled Thermoelasticity of Axially Symmetric Cylindrical Shells," *Journal of Thermal Stresses*, Vol. 17, No. 1, 1994, pp. 115–135.

[8]Shakeri, M., Eslami, M. R., Ghassaa, M., and Ohadi, A. R., "Cylindrical Shells Under Impact Loads Including Transverse Shear and Normal Stress," *Proceedings of the 12th International Conference on Structural Mechanics in Reactor Technology (SMIRT)*, Vol. J, Univ. of Stuttgart, Stuttgart, Germany, 1993, pp. 121–126.

[9]Eslami, M. R., Shakeri, M., Ohadi, A. R., Yas, M. H., and Barzekar, A. R., "Consideration of Normal Stress in Shell Equations Under Shock Loads," *Proceedings of the ASME Engineering System Design and Analysis (ESDA) Conference*, Vol. 8, Pt. B, American Society of Mechanical Engineers, New York, 1994, pp. 337–343.

[10]Kraus, H., *Thin Elastic Shells*, Wiley, New York, 1967.

[11]Lord, H. W., and Shulman, Y., "A Generalized Dynamical Theory of Thermoelasticity," *Journal of Mechanics and Physics of Solids*, Vol. 15, No. 5, 1967, pp. 299–309.

[12]Green, A. E., and Lindsay, K. A., "Thermoelasticity," *Journal of Elasticity*, Vol. 2, No. 1, 1992, pp. 1–7.

[13]Eslami, M. R., and Alizadeh, S. H., "Mixed Galerkin Finite Element Analysis of Non-axisymmetrically Loaded Spherical Shells," *Scientia Iranica*, Vol. 1, No. 2, 1994.

[14]Hughes, T. J. R., *The Finite Element Method*, Prentice–Hall, New York, 1987.

[15]Shakeri, M., Eslami, M. R., and Babai, R., "Galerkin Finite Element of Cylindrical Shells Under Impact Loads," *Proceedings of the 6th International Conference on Finite Element Method*, Sydney, Australia, 1991.

[16]Tessler, A., and Saether, E., "A Computationally Viable Higher-Order Theory for Laminated Composite Plates," *International Journal for Numerical Methods in Engineering*, Vol. 31, 1991, pp.1069–1086.

G. A. Kardomateas
Associate Editor